Memorandum
Gemini 8m Telescopes Project

To: Matt M., Rick M., Dave R., Jim O.
From: Doug S.
Date: August 25, 1994
Re: Analysis of Offset Errors on Reconstructed Dithered Images

Overview

The Gemini SRD specifies image quality in terms of 1 hr integrations with the telescope pointing held fixed during exposures. While this type of observing is often used for CCD imaging, the most common observing mode for the infrared cameras will involve dithering the telescope by a few arcseconds between consecutive frames. Raw frames are then registered and coadded through post processing into a single image. Of specific concern is whether or not an AO corrected PSF suffers significant broadening as a result of random displacements with respect to the pixel grid during successive offsets. Accordingly, the purpose of this analysis is to determine how much random offset errors will impact final image quality in reconstructed, AO corrected, dithered images.

Analysis Technique

Artificial images containing Gaussian noise and several stellar PSFs were created to support this analysis. Each PSF is derived from an AO corrected PSF corresponding to 1.6 µm with 50% strehl supplied by Brent (i.e., Gemini's AO performance specification for median seeing conditions). The details of the simulation are as follows:

1. A total of 20 200x200 pixel frames consisting of noise with a Gaussian spectrum were created. The plate scale is 0.02 arcsec pix^{-1}, i.e., equal to that of the infrared imager's highest resolution.

2. Three Airy functions are added to each frame with peak values set at 3 different levels above the background noise.

3. Each raw frame (noise + 3 Airy functions) is offset by 2.5" in the form of a 3x3 raster pattern. A random noise term with mean 0 and rms ε is added to the offsets. The process is iterated until 20 dithered artificial images are generated.

4. Each shifted frame is then passed through a bilinear interpolation routine to expand the effective plate scale to 0.01" per pixel. This step is used to achieve sub-pixel registration accuracy in the final image.

5. From there each frame is passed through a 2D cross correlation routine that automatically registers the frames so that the PSFs are all aligned with respect to the first image plane.

6. Finally, the median value down the registered data cube is evaluated, and the final image is written to disk for subsequent analysis.

A number of details to this process should be mentioned. First the use of an Airy function to parameterize the actual AO corrected PSF was decided upon after Brent sent me a model PSF with a strehl of 50% at 1.6 µm. Figure 1 shows Brent's AO corrected PSF next to an Airy function of appropriate dimensions to approximate the real PSF. The rms difference in the residual of these two functions is ~1%, evaluated out through the first diffraction ring. The greatest difference is in the height of the first diffraction ring which, not surprisingly, contains more energy in the AO PSF than the Airy function approximation. The actual Airy functional form adopted is:

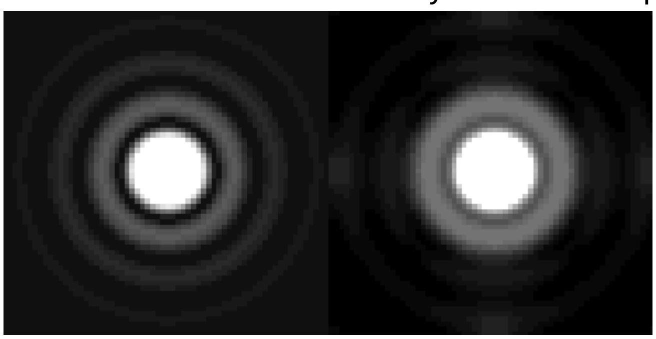

Figure 1 - On the right is the AO corrected PSF supplied by Brent for this analysis, on the left is the Airy function fit to Brent's PSF. The sampling resolution here is 5.5 mas pixel^{-1}. When both functions are scaled to have the same peak value, the rms difference is ~1% out to the first diffraction ring.

$$I(u) = \left(\frac{2J_1(u)}{u} \right)^2$$

where

$$u = w\sqrt{(x_0 - x + \varepsilon_1)^2 + (y_0 - y + \varepsilon_2)^2}$$

and the first order Bessel function $J_1(u)$ is defined in the limiting case:

$$\lim_{u \to 0} \frac{J_1(u)}{u} = \frac{1}{2}$$

Here (x_0, y_0) is the position of the PSF, w is the width of the PSF (1.53 for 0.02" pixels and 50% strehl), and u is simply a running spatial variable. Parameterizing the PSF in analytical form was needed in order to locate the artificial PSF at any sub-pixel location in the images without the uncertainties of binning that using Brent's original PSF would have injected into the analysis. Second, the use of 20 frames with this level of offseting is consistent with a typical high resolution application in which the observer dithers between frames by an amount large enough to avoid overlap in say a distant galaxy (typical dimension of ~1-2”). Third, a median value is calculated instead of a coaddition because that offers the observer the added benefit of eliminating bad pixels from the array without the use of a separate step of interpolating across bad pixels, which can fail for clumps of bad pixels.

If there is a general theme here it is that I am trying to be as realistic as possible in conducting these Monte Carlo simulations, using significant portions of reduction code I have developed over the years to process real infrared array data to handle the image reconstruction.

Results

Figure 2(a) shows a single raw frame with 3 artificial stars in it, with SNRs ranging from 10 to 50. Rms offsetting errors of 0.00, 0.01”, and 0.05” rms were considered in 3 separate Monte Carlo runs. Figure 2(b) shows a reconstructed image, which represents the median of 20 dithered frames. The first diffraction ring is just noticeable surrounding stars 2 and 3. Measured encircled energies in the stellar PSFs for all 3 stars and for the 3 offsetting errors considered are plotted in Figure 3. For star 1 (lowest SNR) there is some evidence of a slight broadening of the PSF for large offset errors (ε = 0.05”). This may be due to the relative weighting of this PSF against the other 2 high SNR PSFs in the 2D cross correlation routine though. For stars 2 and 3, there is no evidence that offsetting errors lead to a loss in image resolution in dithered frames.

This is somewhat contrary to my experience with reconstructing dithered images, in which I generally see a slight degradation after combining many frames. This may be due to:

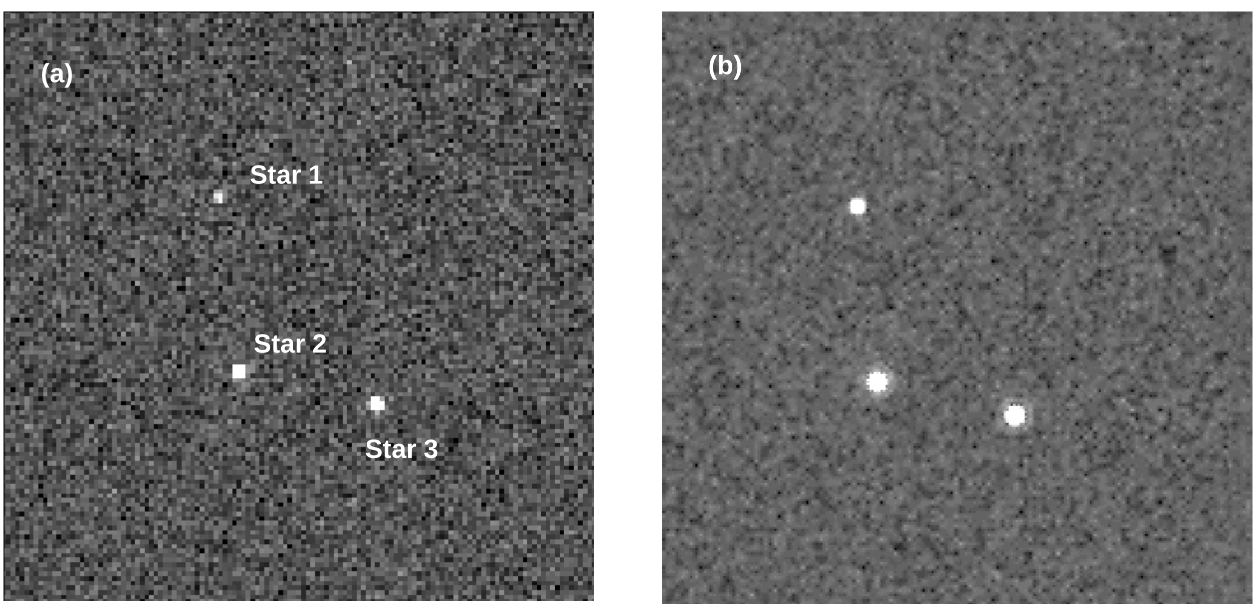

Figure 2(a, b) - Shown in (a) is a single artificial image made with the Gemini infrared imager containing 3 AO corrected stars with 50% strehl and sampled at 0.02 arcsec pix^{-1}. In (b) is the result of reconstructing 20 such images after dithering them in a grid with 2.5” spacing with random errors of 0.05”.

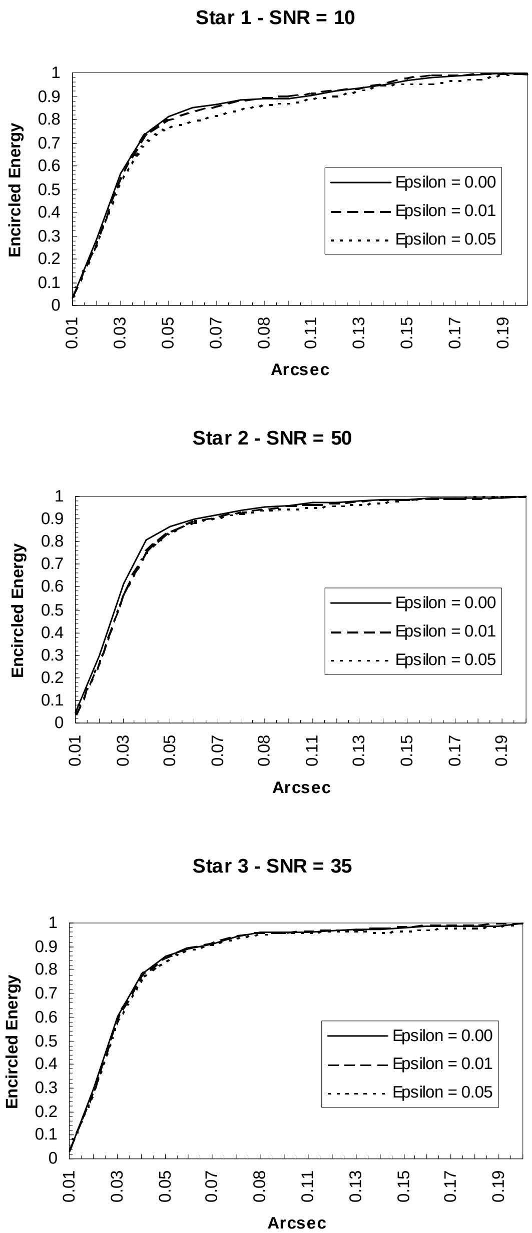

Figure 3 - From top to bottom are encircled energy plots for the stars labeled in Figure 2(a). The factor ε corresponds to the amount of rms error that was allowed during the simulated dither sequence. The encircled energy is essentially independent of ε for stars 2 and 3. There may be a loss in resolution for the faintest star for increasing ε, but this effect could also be due to SNR weighting within the 2D cross correlation program used to reconstruct the images.

1) Variations in seeing during the time an actual dither sequence is acquired.

2) Dead regions between pixels that are typical of infrared arrays. In the NICMOS3 array, for example, a fill factor of ~90-95% is all that is achieved.

Neither of these factors are accounted for in this simulation, which is probably appropriate since the goal here is to isolate A&G offsetting specifications from the other factors that lead to image quality degradation.

Error Tracking Simulation

The current error budget allocation for degradation of the PSF due to image smear (or tracking error during an exposure) is expressed as 0.033" in centroid errors cannot lead to >0.044" boost in the 50% encircled energy of a stellar PSF. In an effort to check that the unique properties of the AO corrected PSF preserve this error budget, a variant of the code used in the previously described analysis was developed. Specifically, tracking error was simulated by creating 1000 frames with the same 50% strehl AO corrected PSF described before, but in this case no dithers were executed. Instead, the frames were shifted by a random amount in X and Y corresponding to Gaussian positional noise with an rms value of 0.033". The median value of the 1000 offset frames was then calculated for each pixel, creating a single smeared image. The simulation was also run for an offsetting error of 0.00" to provide a control measurement. Figure 4(a) shows the simulated image with no offsetting error (i.e., no image smear), and Figure 4(b) shows the same image after applying a tracking error of 0.033" rms during the integration. The peak value drops by a factor of 20 between these images. Figure 5 shows the encircled energy for each image. The width of the 50% encircled energy

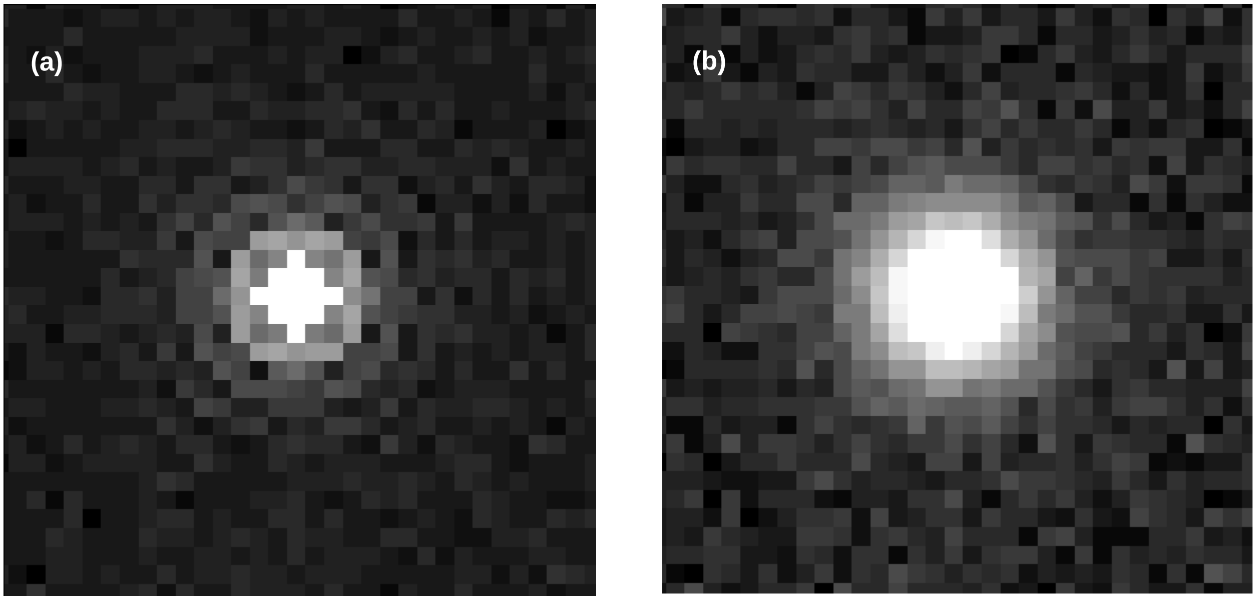

Figure 4(a, b) - On the left in (a) is a an AO corrected image with no tracking error accumulated during the integration. On the right (b) is the same PSF after injecting 0.033” rms tracking error during the integration. The error is assumed to follow Gaussian statistics and be uniformly distributed in terms of radial distance from the center of the PSF. Both images have been expanded to 0.01” per pixel.

point has increased by 0.042” between these images, which is very close to that predicted based upon a simpler analysis previously completed with CODE V and statistical arguments.

Conclusions

Using a realistic PSF and the high resolution imaging mode of the infrared imager I am able to reconstruct without any significant loss in resolution dithered images with varying amounts of offsetting error. In essence this confirms that the 0.02” mode of the infrared imager as a good match for the Gemini AO system. A tracking error analysis reveals the AO corrected encircled energy broadens by 0.042” with 0.033” of tracking error.

In the near future I will also run simulations with a tip/tilt corrected PSFs that Brent will supply in an effort to optimize the other infrared imager plate scales. Please let me know if you would like other simulations run, along the lines described here.

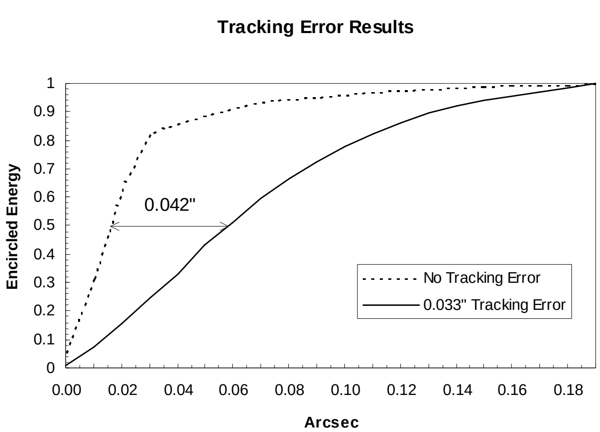

Figure 5 - The encircled energy is plotted for simulated AO corrected PSFs with and without a 0.033” tracking error. The change in encircled energy is 0.042”.